引用格式：YAN Qingze, ZHANG Yixin, ZHU Yun. Transport Properties of Multiple Phase Shift Keying Modulated Perfect Optical Vortex in Turbulent Absorbing Seawater[J]. Acta Photonica Sinica, 2022, 51(11):1106006
闫庆泽,张逸新,朱云.湍流吸收海水中多相移键控调制理想涡旋光子的传输特性[J].光子学报,2022,51(11):1106006

# 湍流吸收海水中多相移键控调制理想涡旋光子的传输特性

闫庆泽,张逸新,朱云
(江南大学 理学院, 江苏 无锡 214122)

**摘　要**:通过建立理想光学涡旋光子所携带轨道角动量模的平均误码概率和信息容量的光传输系统模型,研究了弱湍流光谱吸收海水中多相移键控调制下理想光学涡旋光子的传输特性。基于光传输系统中轨道角动量模的平均误码概率和信息容量模型的数值计算,分析了调制阶和信道参数对理想光学涡旋光子传输的影响。数值研究表明:随着水体虚折射率的增加,光传输系统的平均误码概率和链路信息容量减小。采用更大的环半径和更高的发射功率,可以实现以理想光学涡旋光子为信号载体的水下光传输系统的高信息容量和低平均误码概率的信息传输。最后,通过对该模型的数值分析,得出了平均误码概率和信息容量同时受信号波长和海水吸收系数影响的结论。

**关键词**:理想涡旋光;光学轨道角动量;光谱吸收海水;湍流效应;信息容量;调制
**中图分类号**:TN929.1　　**文献标识码**:A　　**doi**:10.3788/gzxb20225111.1106006

## 0　引言

由于携带轨道角动量(Orbital Angular Momentum ,OAM)的涡旋光束具有宽的传输频带、大的信息传输容量、强抗电磁干扰能力强等优点,涡旋光束在均匀与随机起伏介质中的传输特性已成为光传输领域的热点之一。同时,也引起了水下光传输领域研究人员的关注[1-4]。但是,涡旋光束在海水中传输必然受到海水湍流的扰动产生OAM模间串扰形成噪声,降低涡旋光的传输质量。因此,克服海洋湍流引起的相位干扰,选择和设计通信介质以及研究传输系统的特性迫在眉睫[4-7]。由于海洋湍流是一种无法控制的自然现象,因此,通过光束整形扼制光束衍射和湍流扰动等影响提高涡旋光信号的水下传输能力,已成为当前水下光传输研究领域的重要方向之一。

2013年OSTROVSKY A等[8]首次报道了采用计算机控制液晶空间光调制器产生理想涡旋光(Perfect Optical Vortices, POV), POV光子在海洋湍流中的传输质量主要与光束半径有关,而与波长、拓扑电荷和半径厚度比几乎无关。因此,POV引起了广大研究者的关注。关于理想涡旋光的实验[8]与理论[9]生成及传输特性[10-12]已有大量报道。并且这种新颖的空间结构引起了无湍流自由空间[11-12]、湍流大气[13]和水下[14-15]无线光传输系统研究领域人员的关注。ZHU Fuquan等[11]在2017年通过实验研究了POV光子可以作为水下无线光传输系统的信息载体。SHAO Wei等[12]的研究指出使用POV光子作为传输载体的光传输系统性能比使用Laguerr-Gaussian (LG)光束的光传输系统更好。YANG Chunyong等[13]通过实验证明了大气湍流中POV的传播特性与光束结构整形的设计有关,POV光子的环半径可以有效地改善光传输系统性能。KARAHROUDI M等[14]通过实验讨论了不同水下条件对POV光子传输的影响,并实现了POV光子为载体的高效率海水中的光传输系统。TANG Shanfa等[16]建立了各向异性海洋湍流中POV光子携带的OAM模

**基金项目**:国家自然科学基金(No.61871202)
**第一作者**:闫庆泽(1996—),男,硕士研究生,主要研究方向为光通信。Email:Yanqz0620@163.com
**导师(通讯作者)**:朱云(1977—),女,副教授,博士,主要研究方向为量子光通信、水下光通信。Email: zhuyun1210@163.com
**收稿日期**:2022-04-28;**录用日期**:2022-06-07

态的理论模型。然而，在水下无线光传输系统中，海水的可吸收性是不可忽视的，例如，重庆师范大学吴琼等对水下蓝绿高斯光束的传输过程的蒙特卡洛仿真指出随着海水衰减系数的增加，接收功率将逐渐减小[17]；YANG Hongbin等[18]研究表明海水吸收对POV光子所携带的信号轨道角动量模传输有十分大的衰减作用，并且海水吸收是信号波长的函数[19]。此外，对于光子的调制阶次的差异也影响光子在水下的传输能力[20]。因此，有必要通过研究海水光谱吸收和信号调制阶对POV光子所携带OAM模传播特性的影响。

本文在采用光谱吸收系数描述海水吸收特性的基础上，从POV光子的OAM模的平均误码概率（Average Bit Error Probability，ABEP）和光传输系统信息容量角度，研究海水湍流、吸收和信号多相移键控（Multiple Phase Shift Keying，M-PSK）调制阶对POV传输特性的影响。首先给出了弱湍流的吸收海水中M-PSK调制OAM信号模的ABEP和光传输系统信息容量的理论模，然后数值模拟了ABEP和光传输系统信息容量与湍流参数之间的关系并进行了总结。

## 1 平均误码概率和平均信息容量

在真空中和无湍流空间和柱坐标系$(\rho,\theta,z)$中，POV的复振幅可表示为[11,15]

$$E_{m_0}(\rho,\theta,z)=A_0\frac{\tilde{w}}{w_0(z)}\mathrm{i}^{m_0}\mathrm{J}_{m_0}\left[\frac{2\rho r_0}{\tilde{w}w_0(z)}\exp(\mathrm{i}\Theta_0)\right]\exp\left[-\frac{1}{w_0^2(z)}\left(\rho^2-\left(\frac{zr_0}{z_\mathrm{R}}\right)^2\right)\right]\times \exp\left[\mathrm{i}\left(m_0\theta+\Theta_0+k_0z+k_0\frac{\rho^2+r_0^2}{2R_0(z)}\right)\right] \tag{1}$$

式中，

$$A_0=\frac{1}{\tilde{w}}\sqrt{\frac{2\exp(r_0{}^2/\tilde{w}^2)}{\pi\left|\mathrm{I}_{m_0}(r_0{}^2/\tilde{w}^2)\right|}} \tag{2}$$

式中，$m_0$是初始OAM模的拓扑荷，$\tilde{w}$为POV光子在傅里叶透镜像面处的半宽度，$w_0(z)=\tilde{w}\sqrt{1+z^2/z_\mathrm{R}^2}$，$r_0$是POV在傅里叶透镜物平面处环半径，$\mathrm{J}_{m_0}$是$m_0$阶第一类贝塞尔函数，$\Theta_0=\mathrm{aretan}(z/z_\mathrm{R})$，$k_0=2\pi/\lambda_0$，$\lambda_0$为光在真空中的波长，$R_0(z)=z+z_\mathrm{R}^2/z$，和$z_\mathrm{R}=k_0\tilde{w}^2/2$是瑞利范围，$\mathrm{I}_{m_0}(\cdot)$为第二类$m_0$阶贝塞尔函数。

在弱闪烁湍流[14]、吸收性海水和近轴区域传输的条件下，由湍流像差的相屏近似，POV的复振幅可被表示为[16]

$$E_\mathrm{m}(\rho,\theta,z)\approx E_{\mathrm{om}_0}(\rho,\theta,z)\exp[\mathrm{i}S(\rho,\theta,z)] \tag{3}$$

式中，

$$E_{\mathrm{om}_0}(\rho,\theta,z)=A_0\frac{\tilde{w}}{w(z)}\mathrm{i}^{m_0}\mathrm{J}_{m_0}\left[\frac{2\rho r_0}{\tilde{w}w(z)}\exp(\mathrm{i}\Theta)\right]\exp(\mathrm{i}m_0\theta+\mathrm{i}\Theta+\mathrm{i}k_0n_\mathrm{R}z)\exp\left(\frac{\mathrm{i}k_0n_\mathrm{R}z}{2R(z)}(\rho^2+r_0{}^2)\right)\times \exp\left[-k_0n_\mathrm{I}z\left(1+\frac{\rho^2+r_0{}^2}{2R(z)}\right)\right]\exp\left[-\frac{\rho^2-(zr_0/z_{o\mathrm{R}})^2}{w^2(z)}\right] \tag{4}$$

式中，$S$为湍流相屏引起的零均值高斯随机变量，$w(z)=\tilde{w}\sqrt{1+z^2/z_{o\mathrm{R}}^2}$，$z_{o\mathrm{R}}=k_0\sqrt{n_\mathrm{R}^2+n_\mathrm{I}^2}\,\tilde{w}^2/2$为吸收海水中POV的瑞利范围，$\Theta=\mathrm{aretan}(z/z_{o\mathrm{R}})$，$n_\mathrm{R}$和$n_\mathrm{I}$分别为$n_{oc}$实部和虚部。$n_\mathrm{I}$通过$n_\mathrm{I}=\lambda c_{\mathrm{oc}}/(4\pi)$[21]计算，$c_{\mathrm{oc}}$为海水的平均吸收系数，$R(z)=z+z_{o\mathrm{R}}^2/z$。

由波迭加理论，式(3)中的随机复振幅可由一组标准正交平面螺旋基[22]的叠加给出

$$E_\mathrm{m}(\rho,\theta,z)=\sum_m\alpha_m(\rho,z)\exp(\mathrm{i}m\theta) \tag{5}$$

式中，$m$为湍流海水中的OAM新拓扑荷，$\alpha_m(\rho,z)$是展开系数，可表示为[25]

$$\alpha_m(\rho,z)=\frac{1}{2\pi}\int_0^{2\pi}E_\mathrm{m}(\rho,\theta,z)\exp(-\mathrm{i}m\theta)\mathrm{d}\theta \tag{6}$$

OAM模的条件概率分布$p(m/m_0)$由$\alpha_m(\rho,z)\alpha_m^*(\rho,z)$的湍流系综统计平均值$\langle\alpha_m(\rho,z)\alpha_m^*(\rho,z)\rangle$给出

$$p(m/m_0)=\frac{1}{4\pi^2}\int_0^{2\pi}\int_0^{2\pi}E_{\mathrm{om}_0}(\rho,\theta,z)E^{*}_{\mathrm{om}_0}(\rho,\theta',z)\exp\left[-\frac{1-\cos(\theta-\theta')}{\rho_{\mathrm{o}}^2}2\rho^2\right]\exp\left[-\mathrm{i}m(\theta-\theta')\right]\mathrm{d}\theta\mathrm{d}\theta' \tag{7}$$

式中，$\rho_{\mathrm{o}}$是平面波的横向空间相干半径，其表达式为[23-25]

$$\rho_{\mathrm{o}}=\left\{\frac{9.444C^2_{\varepsilon\chi_{\mathrm{T}}}(n_{\mathrm{R}}^2+n_{\mathrm{I}}^2)z}{\lambda^2(1-\varpi)^2}\left[\varpi^2\kappa_0^{1/3}\mathrm{U}\left(2;\frac{7}{6};\frac{\kappa_0^2\eta^2}{R_{\mathrm{T}}^2}\right)+\varpi^2 4.6\eta^{2/3}\kappa_0\Gamma\left(\frac{7}{3}\right)\mathrm{U}\left(\frac{7}{3};\frac{3}{2};\frac{\kappa_0^2\eta^2}{R_{\mathrm{T}}^2}\right)\kappa_0^{1/3}\mathrm{U}\left(2;\frac{7}{6};\frac{\kappa_0^2\eta^2}{R_{\mathrm{S}}^2}\right)+\right.\right.$$
$$\left.\left.4.6\eta^{2/3}\kappa_0\Gamma\left(\frac{7}{3}\right)\mathrm{U}\left(\frac{7}{3};\frac{3}{2};\frac{\kappa_0^2\eta^2}{R_{\mathrm{S}}^2}\right)-2\varpi\kappa_0^{1/3}\mathrm{U}\left(2;\frac{7}{6};\frac{\kappa_0^2\eta^2}{R_{\mathrm{TS}}^2}\right)-9.2\varpi\eta^{2/3}\kappa_0\Gamma\left(\frac{7}{3}\right)\mathrm{U}\left(\frac{7}{3};\frac{3}{2};\frac{\kappa_0^2\eta^2}{R_{\mathrm{TS}}^2}\right)\right]\right\}^{-1/2} \tag{8}$$

式中，$C^2_{\varepsilon\chi_{\mathrm{T}}}=0.809\times10^{-7}\varepsilon^{-1/3}\chi_{\mathrm{T}}\varpi^{-2}(1-\varpi)^2\left(\mathrm{K}^2/\mathrm{m}^{2/3}\right)$是海洋湍流盐度-温度波动的结构常数，$\varepsilon$是流体单位质量动能耗散率函数，范围为$[10^{-10},10^{-1}]\ \mathrm{m}^2/\mathrm{s}^3$，$\chi_{\mathrm{T}}$是均方温度耗散率函数，范围是$[10^{-10},10^{-2}]\mathrm{K}^2/\mathrm{s}$，$\varpi$是温度和盐度波动对折射率谱的贡献之比，折射率谱可在区间$(-5,0)$内变化。当$\varpi=-5$时，温度波动对光学湍流的诱导起主导作用，当$\varpi=0$时，盐度波动对光学湍流的诱导起主导作用。$\kappa$为湍流涨落的标量空间波数，$\kappa_0=2\pi/L_0$，$\kappa_{\mathrm{T}}=R_{\mathrm{T}}/\eta$，$\kappa_{\mathrm{S}}=R_{\mathrm{S}}/\eta$，$\kappa_{\mathrm{TS}}=R_{\mathrm{TS}}/\eta$，$\eta$为湍流内尺度，$L_0$为湍流外尺度，$R_j=\sqrt{3}\left[W_j-\frac{1}{3}+(9W_j)^{-1}\right]^{3/2}Q^{-3/2}$（$j=\mathrm{T},\ \mathrm{S},\ \mathrm{TS}$），$W_j=\left\{\left[\frac{P_{\mathrm{r}j}^2Q^4}{(6\beta)^2}-\frac{P_{\mathrm{r}j}Q^2}{81\beta}\right]^{1/2}-\left[\frac{1}{27}-\frac{P_{\mathrm{r}j}Q^2}{6\beta}\right]\right\}^{1/3}$，$Q$为无量纲常数，$P_{\mathrm{rT}}$和$P_{\mathrm{rS}}$分别表示温度和盐度的普朗特数，$P_{\mathrm{rTS}}=2P_{\mathrm{rT}}P_{\mathrm{rS}}/(P_{\mathrm{rT}}+P_{\mathrm{rS}})$，$\mathrm{U}(\cdot)$是第二类合流超几何函数。

由式(1)～(7)，经过运算可得

$$\begin{aligned}p(m/m_0)=&\frac{1}{4\pi^2}\left(\frac{A_0\tilde{w}}{w(z)}\right)^2\left|\mathrm{J}_{m_0}\left[\frac{2\rho r_0}{\tilde{w}w(z)}\right]\right|^2\exp\left[-2k_0n_{\mathrm{I}}z\left(1+\frac{r_0^{\ 2}}{2R(z)}\right)\right]\times\\&\exp\left[-\left(\frac{1}{w^2(z)}+\frac{1}{\rho_{\mathrm{o}}^2}+\frac{k_0n_{\mathrm{I}}z}{2R(z)}\right)2\rho^2\right]\exp\left[\frac{8(zr_0)^2n_{\mathrm{R}}^2}{w^2(z)k_0^2\tilde{w}^4\left(n_{\mathrm{R}}^2+n_{\mathrm{I}}^2\right)^2}\right]\times\\&\int_0^{2\pi}\int_0^{2\pi}\exp\left[-\mathrm{i}(m-m_0)(\theta-\theta')\right]\exp\left[\frac{2\cos(\theta-\theta')\rho^2}{\rho_{\mathrm{o}}^2}\right]\mathrm{d}\theta\mathrm{d}\theta'\end{aligned} \tag{9}$$

考虑到积分关系[26]

$$\int_0^{2\pi}\exp\left[\tau\cos(\theta-\phi)-\mathrm{i}m\theta\right]\mathrm{d}\theta=2\pi\mathrm{I}_m(\tau)\exp(-\mathrm{i}m\phi) \tag{10}$$

由式(9)和(10)，可得POV发射模为拓扑荷$m_0$时的条件概率分布

$$\begin{aligned}p(m/m_0)=&\left(\frac{A_0\tilde{w}}{w(z)}\right)^2\exp\left[-2k_0n_{\mathrm{I}}z\left(1+\frac{r_0^{\ 2}}{2R(z)}\right)\right]\exp\left[\frac{8(zr_0)^2n_{\mathrm{R}}^2}{w^2(z)k_0^2\tilde{w}^4\left(n_{\mathrm{R}}^2+n_{\mathrm{I}}^2\right)^2}\right]\times\\&\exp\left(-\frac{\rho^2}{w_{\mathrm{eff}}^2}\right)\left|\mathrm{J}_{m_0}\left[\frac{2\rho r_0}{\tilde{w}w(z)}\right]\right|^2\mathrm{I}_{m-m_0}\left[\frac{2\rho^2}{\rho_{\mathrm{o}}^2}\right]\end{aligned} \tag{11}$$

式中，$w_{\mathrm{eff}}=\left(\frac{2}{w^2(z)}+\frac{2}{\rho_{\mathrm{o}}^2}+\frac{k_0n_{\mathrm{I}}z}{R(z)}\right)^{-1/2}$为被吸收的海水湍流中POV的有效半径，$\mathrm{I}_m(\cdot)$为第二类$m$阶贝塞尔函数。

接收器接收到的POV的OAM模的接收概率可表示为

$$P(m|m_0)=2\pi\int_0^{D/2}p(m|m_0)\rho\mathrm{d}\rho \tag{12}$$

式中，$D$为接收半径。

当$m\neq m_0$，$P(m|m_0)_{m\neq m_0}$为OAM串扰模式的概率，描述了光子从OAM信号模跃迁到新的OAM模的

概率，当$m=m_0$，$P\left(m|m_0\right)_{m=m_0}$为OAM信号模的概率。

OAM信道的平均信号-串音-噪声比为[27-28]

$$\gamma_{m,m_0}=\frac{P\left(m/m_0\right)_{m=m_0}}{\sum_{m=-\infty}^{\infty}P\left(m/m_0\right)_{m\neq m_0}+N_0/P_{\mathrm{TX}}} \tag{13}$$

式中，$\sum_{m=-\infty}^{\infty}P\left(m/m_0\right)_{m\neq m_0}$表示从信号模跃迁到其他彼此独立OAM模的功率。$P_{\mathrm{TX}}$为发射功率，$N_0$为接收噪声功率。

对于M-PSK调制下的信号调制，基于式(13)，导出第$m$个OAM信道的ABEP为[29]

$$p_{\mathrm{M-PSK}}\approx\frac{2}{\log_2 M}\mathrm{erfc}\left(\sqrt{\gamma_{m,m_0}\log_2 M}\sin\frac{\pi}{M}\right) \tag{14}$$

式中，erfc(·)为余误差函数，$M$为调制阶次，$p_{\mathrm{M-PSK}}$描述了系统接收端接收到正确信号和发射总信号的比。

假设星座点用格雷码标记，符号错误仅造成符号组成的$\log_2 M$位中的1位损坏[32]，M-PSK的符号错误概率表示为

$$p_{\mathrm{SM-PSK}}\approx 2\mathrm{erfc}\left(\sqrt{\gamma_{m,m_0}\log_2 M}\sin\frac{\pi}{M}\right) \tag{15}$$

对于$N=2m+1$输入和$N=2m+1$输出的对称性OAM信道，$X=\{m_{00},m_{01},\cdots,m_{0\mathrm{l}-1}\}$和$Y=\{m_0,m_1,\cdots,m_{T-1}\}$分别代表信号输入和信号输出，可以分别得到$p\left(m_t|m_{0i}\right)=P_{\mathrm{SM-PSK}}/(M-1)$和$P_{\mathrm{SM-PSK}}$，其中$p\left(m_t|m_{0i}\right)=P_{\mathrm{SM-PSK}}/(M-1)$表示符号错误概率。由此光传输系统的平均信息容量可表示为[29]

$$C=\log_2 N+(1-p_{\mathrm{SM-PSK}})\log_2(1-p_{\mathrm{SM-PSK}})+p_{\mathrm{SM-PSK}}\log_2\frac{p_{\mathrm{SM-PSK}}}{N-1} \tag{16}$$

利用式(15)和式(16)，可得出M-PSK调制光传输系统的平均信息容量式(17)，即

$$\begin{aligned}C_{\mathrm{M-SPK}}=&\log_2 N+\left(1-2\mathrm{erfc}\left(\sqrt{\gamma_{m,m_0}\log_2 M}\sin\frac{\pi}{M}\right)\right)2\mathrm{erfc}\left(\sqrt{\gamma_{m,m_0}\log_2 M}\sin\frac{\pi}{M}\right)+\\&2\mathrm{erfc}\left(\sqrt{\gamma_{m,m_0}\log_2 M}\sin\frac{\pi}{M}\right)\log_2\frac{2\mathrm{erfc}\left(\sqrt{\gamma_{m,m_0}\log_2 M}\sin\frac{\pi}{M}\right)}{N-1}\end{aligned} \tag{17}$$

式中，$N=-m,-m+1,\cdots,0,\cdots,m-1,m$，平均信息容量代表光传输系统接收端的最大数据速率。

## 2 数值分析

通过对M-PSK调制POV光子所携带的OAM模的ABEP和光学系统平均信息容量理论模型的数值计算来分析湍流吸收海水中调制理想涡旋光子的传输特性。在数值计算中，采用湍流模型特征参数[23]$P_{\mathrm{rT}}=0.72$，$P_{\mathrm{rS}}=700$，$Q=2.5$和目前水下光传输实验能实现的最长传输距离$z=200\ \mathrm{m}$[30]。此外，除非特殊说明，采用光束和湍流参数：$r_0=0.03\ \mathrm{m}$，$C_{\varepsilon\chi_{\mathrm{T}}}^2=10^{-13}\ \mathrm{K^2/m^{2/3}}$($\varepsilon=10^{-3}\ \mathrm{m^2/s^3}$，$\varpi=-4.5$，$\chi_{\mathrm{T}}=10^{-7}\ \mathrm{K^2/s}$)，$\tilde{w}=0.003\ \mathrm{m}$，$\eta=0.001\ \mathrm{m}$，$L_0=10\ \mathrm{m}$，$m_0=1$，$n_1=0.448\ 7\times10^{-9}$($\lambda=470\ \mathrm{nm}$)，$D=0.03\ \mathrm{m}$.

图1为吸收湍流海水中M-PSK调制POV光子的OAM信号模的平均误码率和光传输系统信息容量与传输距离间的关系。其中数值曲线首先表示，当POV光子的传输距离增加时，接收到的OAM信号ABEP也随之增加，而光传输系统的信息容量由随之减小。这是因为随着POV光子在湍流海水中传输距离的增加，海水湍流所产生的相差逐步增加，使得OAM信号模从原来的轨道角动量能级跃迁临近的轨道角动量能级的概率增加，从而测得OAM信号模的概率降低和ABEP增加，导致光学系统传输信号信息的能力降低。此外，海水的吸收也是降低OAM信号模接收概率和增加ABEP的因素之一。图1给出了不同调制阶$M$对应的数值曲线。当POV光子最大传输距离$z=200\ \mathrm{m}$时，选用M-PSK的调制阶$M=Q=4$是最佳选择，此结果表示在进行信号调制时应该注意调制阶的阶次$M$。因此在之后的研究中调制方式选择使用QPSK，即4-PSK。

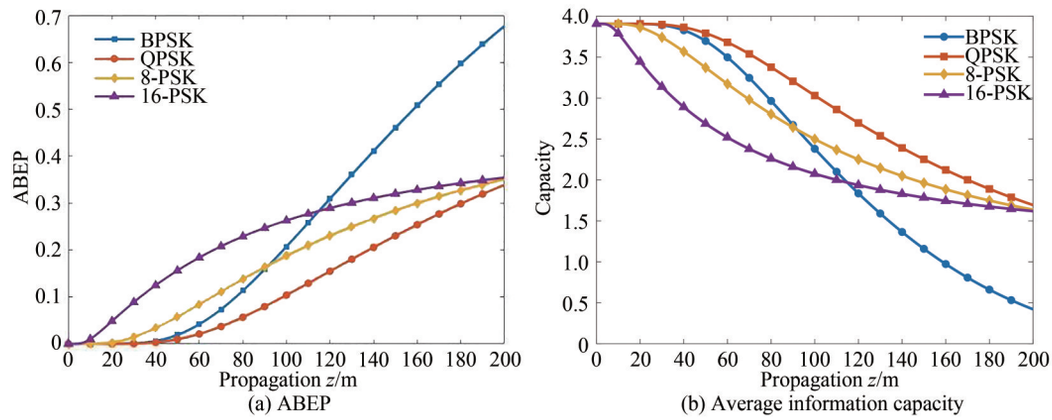


图1　OAM信号模的ABEP和信息容量与传播距离的关系

Fig. 1　The relationship between the ABEP and the average information capacity and the propagation distance

如图2所示，研究了四种吸收海水（纯海水$\lambda=410$ nm（$n_{\mathrm{I}}=0.358\ 8\times10^{-9}$），清澈海水$\lambda=470$ nm（$n_{\mathrm{I}}=0.448\ 7\times10^{-9}$），沿海海水$\lambda=510$ nm（$n_{\mathrm{I}}=1.054\ 9\times10^{-9}$）and 浑浊海水$\lambda=570$ nm（$n_{\mathrm{I}}=3.401\ 0\times10^{-9}$）[31]）对QPSK调制POV的OAM信号光子的ABEP和光传输系统信息容量的影响，其中波长410 nm对应的虚折射率$n_{\mathrm{I}}=0.358\ 8\times10^{-9}$，470 nm对应的虚折射率$n_{\mathrm{I}}=0.448\ 7\times10^{-9}$，510 nm对应的虚折射率$n_{\mathrm{I}}=1.054\ 9\times10^{-9}$，570 nm对应的虚折射率$n_{\mathrm{I}}=3.401\ 0\times10^{-9}$。可知，随着传输距离和海水吸收率的增加，系统的信息量减小，ABEP增大。在100 m范围内传输时，吸收介质越大，系统的信息量越大，ABEP越小。这是因为信号波长较短，海水吸收对信号的衰减小于波长增加对信号传输的影响。但随着传输距离的进一步增加，吸收占据了主导地位。这是由于长波长的光束更容易受到湍流的影响，随着距离的增加，吸收变得更明显。因此，海水吸收是海水中光子传输不可忽视的一部分。

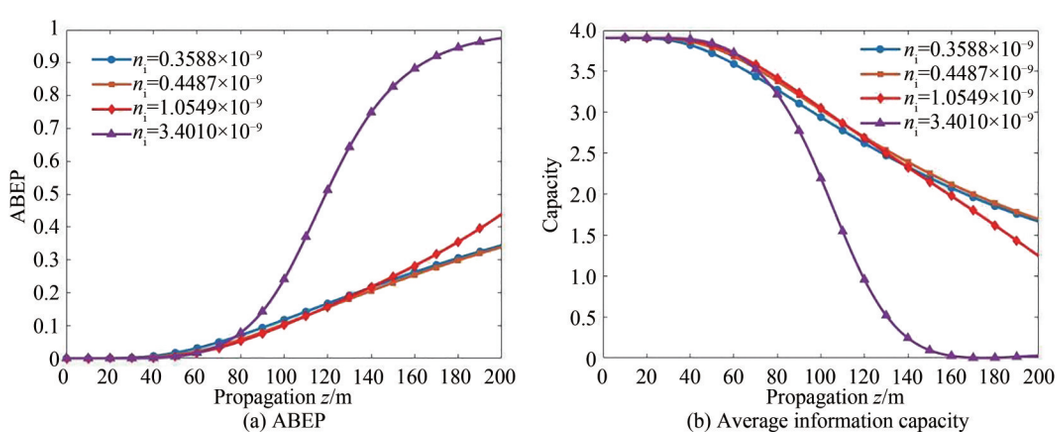


图2　OAM信号模的ABEP和信息容量与传播距离间的关系

Fig. 2　The relationship between the ABEP and the average information capacity and the propagation distance of OAM mode

图3为QPSK调制POV的OAM信号模的ABEP和光传输系统信息容量与理想光涡旋的环半径之间的关系。可以发现，随着湍流强度的增加，信号模的ABEP增加而光传输系统信息容量降低。这是因为随着海水湍流强度的增加，湍流对传输POV光子的干扰程度也增强，致使OAM信号模从原来的轨道角动量能级跃迁到临近轨道角动量能级的概率增加，从而构成OAM串音概率和OAM信号模的ABEP增加，导致光传输系统传输信号信息的能力降低。随着POV的环半径的增大，ABEP减小，而信息容量增大。并且随POV的环半径的增大存在与湍流强度相关的ABEP降低和信息量增大的稳定区。例如，当$C_{\varepsilon\chi_{\mathrm{T}}}^2=5\times10^{-15}\ \mathrm{K^2/m^{2/3}}$时，$r_0=0.010$ m，系统的信息容量和ABEP都接近稳定值，而当$C_{\varepsilon\chi_{\mathrm{T}}}^2=10^{-14}\ \mathrm{K^2/m^{2/3}}$时，$r_0=0.015$ m，系统信息容量和ABEP都接近稳定值。因此，在湍流强度更大时，相应的调整POV环半径可以减小因湍流带来的系统信息容量的衰减和ABEP的增加。

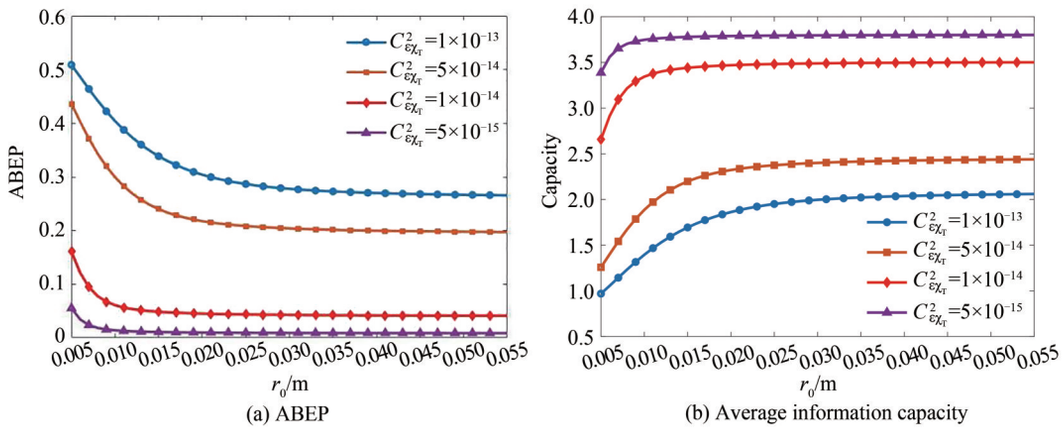


图3 OAM信号模的ABEP和信息容量与理想光涡环半径的关系

Fig. 3 The relationship between the ABEP and average information capacity of the OAM mode and the ideal vortex ring radius

图4描述了温度和盐度波动比和收发光学系统信噪比$P_{TX}/N_0$与QPSK调制POV的OAM信号模的ABEP和光传输系统信息容量的关系。由图4可以直观的发现，随着$\varpi$的增大，水下光信号传输系统的信息量增大，而ABEP减小，此结果与已有类似研究是一致的[18]。图4给出的更有价值的结果是收发光学系统的$P_{TX}/N_0$越大，光传输系统能够传输的信息容量越大，而其ABEP越小。这很容易理解，收发光学系统的$P_{TX}/N_0$越大，光传输系统的噪声就低。此结果表明，提高收发光学系统的信噪比是改善POV光传输系统的ABEP和信息容量的办法之一。

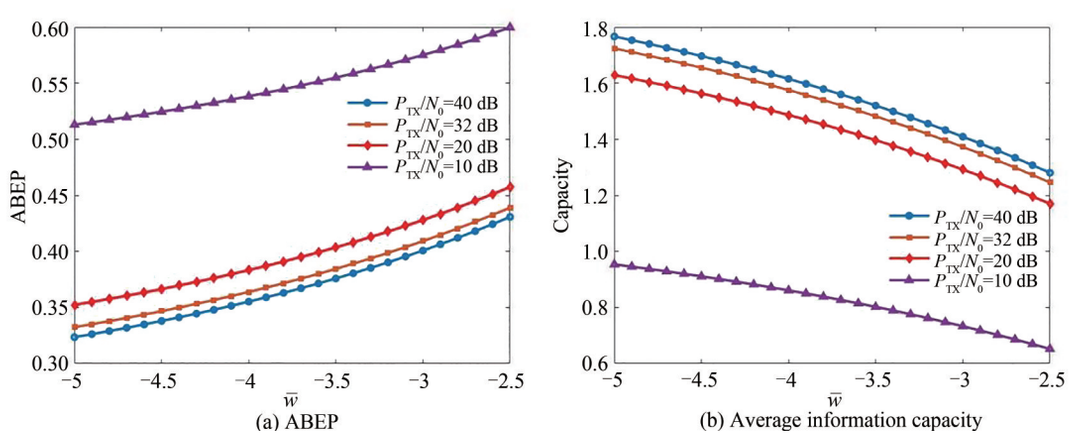


图4 OAM信号模的ABEP和信息容量与温度和盐度波动比的关系

Fig. 4 The ABEP and average information capacity versus the ratio of temperature and salinity fluctuation

如图5所示，QPSK调制POV的OAM信号模的ABEP和光传输系统信息容量随海水湍流内外尺度的变化而变化。可知，光传输系统的信息容量随着海水湍流外尺度的增大而减小，随着海水湍流内尺度的减小而减小。ABEP的变化趋势与光传输系统的信息容量的变化趋势相反。这是因为湍流的外尺度主要导致光束传播路径的随机偏转。外尺度越大，波束漂移越大，接收端信号的接收概率越小。因此，对于湍流外尺度较大的通道，随机偏转越大，任意垂直于光轴的平面中构成OAM模的随机子光束间的光程差就越大，即OAM模的波前畸变也很大，产生串扰随之增大，使得ABEP增大，光传输系统的信息容量减小。另一方面，随着湍流内尺度的增大，穿过光束截面的海水均匀区域增大，OAM信号模的波前失真减小，即OAM信号模的透射率增大。

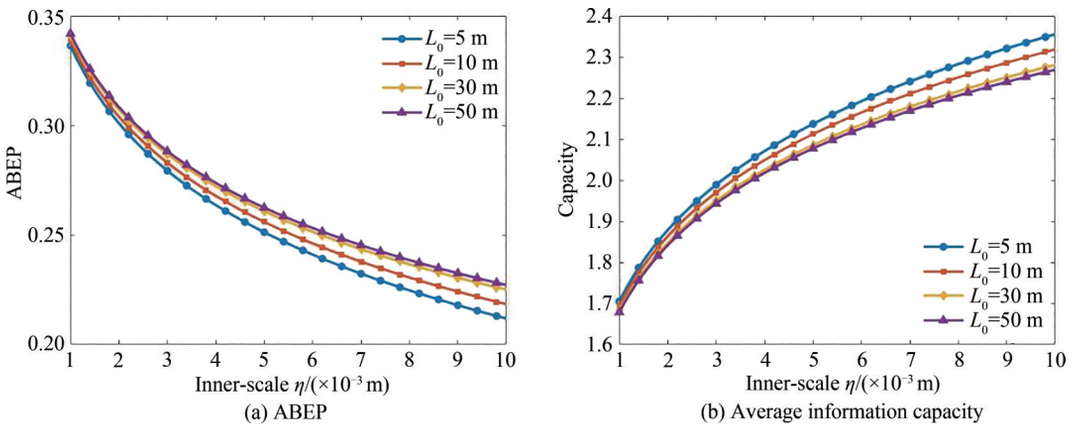


图5　OAM信号模的ABEP和信息容量与湍流内外尺度间的变化

Fig. 5　The ABEP and information capacity versus the inner-scale $\eta$ of turbulence for the difference outer-scale $L_0$

## 3　结论

本文推导了在吸收型湍流海水中传输的POV的OAM信号模的ABEP和光传输系统的信息容量的模型。结果表明，在传输距离小于100 m时，POV的OAM信号模的波长对传输系统的信息容量的影响大于海水吸收，而当传输距离在100～200 m之间时，海水吸收对光传输系统的信息容量的影响大于波长。当理想光涡旋的环半径$r_0$增大时，系统的信息容量也增大，并且ABEP减小，但随着POV环半径的增大存在与湍流强度相关的ABEP降低和信息容量增大的稳定区。接收和发射光学系统信噪比的增大会使系统的信息容量增大和ABEP减小。湍流内尺度的增加和湍流外尺度的减少也有助于系统信息容量的增加和ABEP的降低。此外，QPSK调制下的POV的OAM信号模在吸收弱湍流链路中受到的影响小于其他阶次的调制。因此，在选择合适的调制方案的基础上，适当增大理想涡旋光子的环半径及增加收发光学系统信噪比，可以有效提高POV的OAM信号光子的信息携带能力。

**参考文献**

[1] XIAO Weiwei, ZHANG Han, ZHAO Xinying, et al. Propagation property of X-type vortex beam under the interaction of SAM and OAM[J]. Acta Photonica Sinica, 2022, 51(1): 0151115.
肖维维，张晗，赵馨颖，等. 自旋-轨道相互作用下X型涡旋光束的传播特性[J]. 光子学报，2022，51(1)：0151115.

[2] CHENG Mingjian, GUO Lixin, LI Jiangting, et al. Channel capacity of the OAM based free-space optical communication links with Bessel-Gauss beams in turbulent ocean[J]. IEEE Photonics Journal, 2016, 8(1): 7901411.

[3] LI Ye, YU Lin, ZHANG Yixin. Influence of anisotropic turbulence on the orbital angular momentum modes of Hermite-Gaussian vortex beam in the ocean[J] Optics Express, 2017, 25(11): 12203-12215.

[4] CUI Xiaozhou, YIN Xiaoli, CHANG Huan, et al. Analysis of an adaptive orbital angular momentum shift keying decoder based on machine learning under oceanic turbulence channels[J] Optics Communication, 2018, 429(15): 138-143.

[5] WILLNER A, ZHAO Zhe, REN Yongxiong, et al. Underwater optical communications using orbital angular momentum-based spatial division multiplexing[J] Optics Communication, 2018, 408(1): 21-25.

[6] YU Lin, ZHANG Yixin. Analysis of modal crosstalk for communication in turbulent ocean using Lommel-Gaussian beam[J] Optics Express, 2017, 25(19): 22565-22574.

[7] DENG Shibao, YANG Dongyu, ZHANG Yixin. Capacity of communication link with carrier of vortex localized wave in absorptive turbulent seawater[J]. Waves in Random and Complex Media, 2020: 1844925.

[8] OSTROVSKY A, RICKENSTORFF-PARRAO C, ARRIZÓN V. Generation of the 'perfect' optical vortex using a liquid-crystal spatial light modulator[J] Optics Letters, 2013, 38(4): 534-536.

[9] LIANG Yansheng, YAN Shaohui, HE Minru, et al. Generation of a double-ring perfect optical vortex by the Fourier transform of azimuthally polarized Bessel beams[J] Optics Letters, 2019, 44(6): 1504-1508.

[10] PINNELL J, RODRÍGUEZ-FAJARDO V, FORBES A. How perfect are perfect vortex beams?[J] Optics Letters, 2019, 44(22): 5614-5617.

[11] ZHU Fuquan, HUANG Sujuan, SHAO Wei, et al. Free-space optical communication link using perfect vortex beams carrying orbital angular momentum (OAM)[J]. Optics Communication, 2017, 396(1): 50-57.

[12] SHAO Wei, HUANG Sujuan, LIU Xianpeng, et al. Free-space optical communication with perfect optical vortex beams multiplexing[J] Optics Communication, 2018, 427(15): 545-550.

[13] YANG Chunyong, LAN Yue, JIANG Xiaoyu, et al. Beam-holding property analysis of the perfect optical vortex beam transmitting in atmospheric turbulence[J]. Optics Communication, 2020, 472(1): 125879.
[14] KARAHROUDI M, MOOSAVI S A, MOBASHERY A, et al. Performance evaluation of perfect optical vortices transmission in an underwater optical communication system[J]. Applied Optics, 2018, 57(30): 9148-9154.
[15] WANG Wei, WANG Ping, PANG Weina, et al. Evolution properties and spatial-mode UWOC performances of the perfect vortex beam subject to oceanic turbulence[J]. IEEE Transactions on Communicayions, 2021, 69(11): 7647-7658.
[16] TANG Shanfa, YAN Jiawei, YONG Kangle, et al. Propagation characteristics of the perfect vortex beam in anisotropic oceanic turbulence[J]. Applied Optics, 2020,59(32): 9956-9962.
[17] WU Qiong, WANG Bo, WANG Tao, et al. Analysis of underwater wireless optical transmission characteristics based on Monte Carlo method[J]. Acta Photonica Sinica, 2021, 50(4): 0406002.
吴琼, 王博, 王涛, 等. 基于蒙特卡洛法的水下无线光传输特性分析[J]. 光子学报, 2021, 50(4): 0406002.
[18] YANG Hongbin, YAN Qingze, ZHANNG Yixin, et al. Received probability of perfect optical vortex in absorbent and weak turbulent seawater links[J] Applied Optics, 60(35): 10772-10779.
[19] ZHU Yun, ZHANG Yixin, HU Zhengda. Spiral spectrum of Airy beams propagation through moderate-to-strong turbulence of maritime atmosphere[J]. Optics Express, 2016 , 24(10): 10847-10857.
[20] JEONG G, KIM S. Performance evaluation of underwater optical wireless communication depending on the modulation scheme[J]. Current Optics and Photonics, 2022,6(1): 39-43.
[21] FEWELL M, TROJAN A. Absorption of light by water in the region of high transparency: recommended values for photon-transport calculations[J]. Applied Optics. 2019, 58(9): 2408-2421.
[22] YAN Qingze, ZHU Yun, ZHANG Yixin. Capacity of the weakly absorbent turbulent ocean channel with the coaxial double-position power Gaussian vortex[J]. Journal of Marine Science and Engineering, 2021, 9(10): 111712-111717.
[23] LI Ye, ZHANG Yinxin, ZHU Yun. Oceanic spectrum of unstable stratification turbulence with outer scale and scintillation index of Gaussian-beam wave[J] Optics Express. 2019,27(5): 16-22.
[24] GUTIÉRREZ-VEGA J, BANDRES M. Normalization of the Mathieu-Gauss optical beams[J]. Journal of the Optical Society of America A, 2007, 24(1): 215-220.
[25] ANDREWS L,PHILLIPS R. Laser beam propagation through random medium[M]. Bellingham: SPIE Press, 2005.
[26] JEFFREY A, ZWILLINGER D. Table of integrals, series, and products[M]. San Diego: Academic, 2007.
[27] HO K. Phase-modulated optical communication systems[M]. New York: Springer, 2001.
[28] YANG Hongbin, YAN Qingze, WANG Pan, et al. Bit-error rate and average capacity of an absorbent and turbulent underwater wireless communication link with perfect Laguerre-Gauss beam[J]. Optics Express, 2022, 30(6): 9053-9064.
[29] KROUK E, SEMENOV S. Modulation and coding techniques in wireless communications[M]. India: Wiley, 2011.
[30] DAI Yizhan, CHEN Xiao, YANG Xingqi, et al. 200-m/500-Mbps underwater wireless optical communication system utilizing a sparse nonlinear equalizer with a variable step size generalized orthogonal matching pursuit[J]. Optics Express, 2021, 29(20): 32228-32243.
[31] WOZ'NIAK B, DERA J. Light absorption in sea water[M]. New York: Springer, 2007.

# Transport Properties of Multiple Phase Shift Keying Modulated Perfect Optical Vortex in Turbulent Absorbing Seawater

YAN Qingze, ZHANG Yixin, ZHU Yun
(*School of Science, Jiangnan University, Wuxi, Jiangsu* 214122, *China*)

**Abstract**: Since Orbital Angular Momentum (OAM) mode can form an infinite *N* qubit basis, it provides a new coding scheme for communication links. However, ocean turbulence and other external disturbances can cause phase disturbance of OAM mode, which generates the cross talk between the energy states of OAM modes. The self-focusing property of POV is beneficial to the transmission of OAM modes. The transmission quality of POV beams in oceanic turbulence is most related to the beam radius, while it is nearly free from the wavelength, topological charge, and radius-thickness ratio. Because of these special characteristics, POV has attracted wide attention of researchers. Moreover, the absorption of seawater reduces the information carrying capacity of POV photons and weakens the reliability of the system. Therefore, it is necessary to study the absorption of seawater and the transmission characteristics of POV. In addition, the modulation of POV also increases the information capacity carried by the POV′s OAM

mode. In this paper, the ABEP and information capacity of underwater optical transmission system based on POV carrier and M-PSK modulation are studied under weak absorption turbulence. The wavelength dependence of fading channel is especially considered. The fading channel consists of two parts: signal energy loss caused by seawater turbulence and seawater absorption. Under the condition of paraxial transmission and Rytov approximation, the closed expressions of mean signal-to-noise ratio and signal error probability for M-PSK OAM channel are derived. Considering that the number of OAM signal level channels in common use is far less than the number of OAM topological charge (energy level) of POV vortex carrier, the concept that POV vortex carrier communication link is a symmetric link composed of multiple OAM level channels is proposed. Using the derived expression of ABEP of M-PSK OAM channel and the concept of symmetric link of multi-OAM channel, a novel closed-form expression of ABER and average capacity under various modulation schemes is proposed. Finally, through numerical analysis of the model, new results are draw. The results show that when transmitting over short distances, the wavelength of the photon of the OAM signal of POV has a greater impact on the information capacity of the transmission system than on the absorption of seawater, while when transmitting over long distances, the effect of seawater absorption on the information capacity of the optical transmission system is greater than the wavelength. When the ring radius of the perfect optical vortex increases, the information capacity of the system also increases, and ABEP decreases, but with the increase of the ring radius of POV there is a stable region of ABEP decrease and information capacity increase related to turbulence intensity. The increase in the signal-to-noise ratio of the receiving and transmitting optical systems results in an increase in the information capacity of the system and a decrease in ABEP. The increase of the inner-scale and the decrease of the outer-scale also lead to the increase the information capacity of the system and the decrease of ABEP. In addition, the OAM signal photons of the POV under QPSK modulation are less affected in absorbing weak turbulence links than other orders of modulation. Therefore, on the basis of selecting the appropriate modulation scheme, the ring radius of the POV and the signal-to-noise ratio of the transceiver optical system, which can effectively enhance the information capacity of the OAM signal photon of the POV.

**Key words**: Perfect optical vortex; Optical orbital angular momentum; Spectral absorption of seawater; Turbulence effect; Information capacity; Modulation

**OCIS Codes**: 050.4865; 010.4455; 060.4080; 060.4510

**Foundation item**: National Natural Science Foundation of China(No.61871202)